

Supplementary Information for:

Oxygen vacancy formation characteristics in the bulk and across different surface terminations of $\text{La}_{(1-x)}\text{Sr}_x\text{Fe}_{(1-y)}\text{Co}_y\text{O}_{(3-\delta)}$ perovskite oxides for CO_2 conversion

Debtanu Maiti¹, Yolanda A. Daza¹, Matthew M. Yung², John N. Kuhn¹ and Venkat R.

Bhethanabotla^{1*}

1. University of South Florida. Tampa, FL 33620

2. National Renewable Energy Laboratory. Golden, CO 80401

Bulk Configurations:

Figure S1 reveals the various bulk configurations of $\text{La}_{0.5}\text{Sr}_{0.5}\text{FeO}_3$ that can exhibit the same cubic structure in XRD techniques. Each of these structures were tested for stability thorough DFT calculated energies. The structures with the minimum energy was chosen as the most stable one.

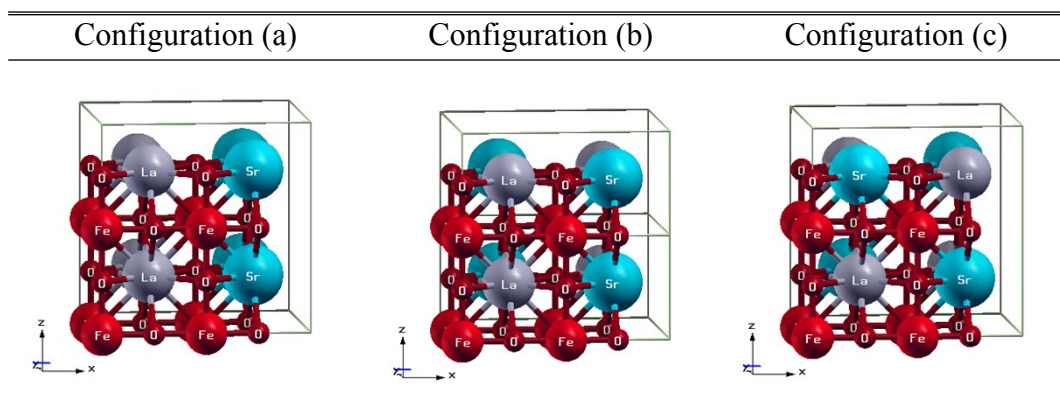


Figure S1: Various bulk phase structural configurations of $\text{La}_{0.5}\text{Sr}_{0.5}\text{FeO}_3$

*Corresponding author email: bhethana@usf.edu

DFT+U Graphs of bulk oxygen vacancy formation energies

The oxygen vacancy formation energies in bulk $\text{La}_{0.5}\text{Sr}_{0.5}\text{CoO}_3$ and $\text{La}_{0.5}\text{Sr}_{0.5}\text{FeO}_3$ were also calculated accounting for the Hubbard U correction. U values of 2, 3 and 4 were used for the purpose. Across all the U values, the trend of increasing oxygen vacancy formation energies for iron-rich 'B' site in comparison to cobalt-rich 'B' site was found to be valid.

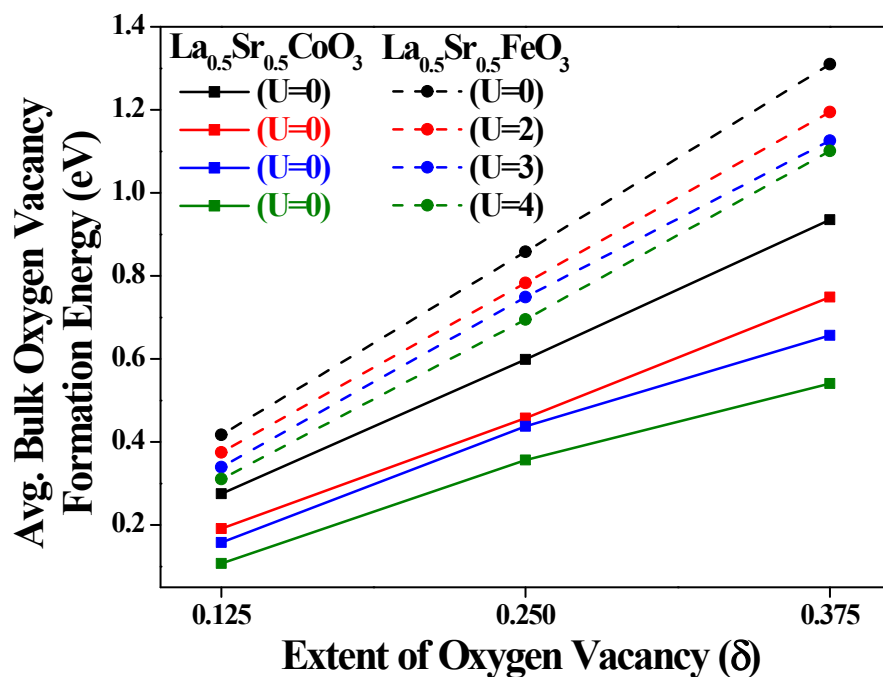


Figure S2. Bulk oxygen vacancy formation energies for $\text{La}_{0.5}\text{Sr}_{0.5}\text{CoO}_3$ and $\text{La}_{0.5}\text{Sr}_{0.5}\text{FeO}_3$ using DFT+U

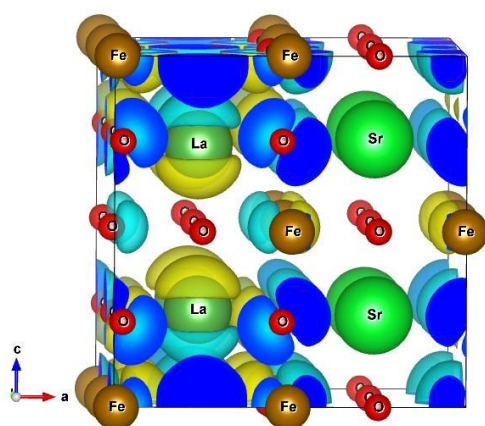
Site specific oxygen vacancy formation in the bulk materials:

Oxygen vacancy formation was dependent on the different sites of the bulk material. Continuous vacancy formation was favored in comparison to distributed vacancy. Figure S3 reveals the charge density difference maps between the pure and oxygen vacant material, for different vacancy formation sites.

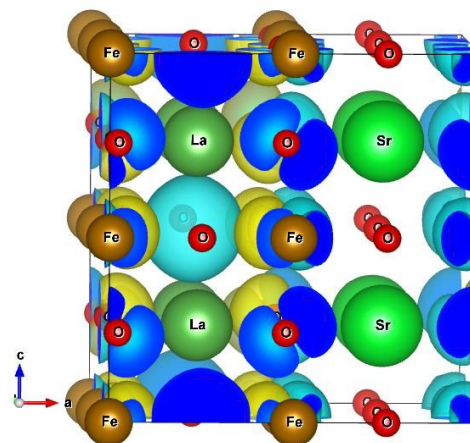
Continuous Vacancy ($\delta=0.25$)

Distributed Vacancy ($\delta=0.25$)

Vacancy formation energies in lanthanum layer

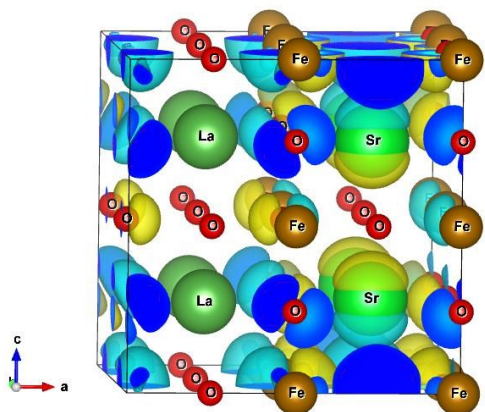


E = 6.3112 eV

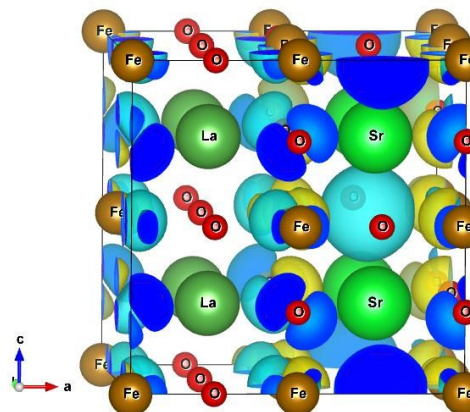


E = 6.9297 eV

Vacancy formation energies in strontium layer



E = 7.1518 eV



E = 7.6579 eV

Figure S3: Charge density difference maps for different oxygen vacancy generation sites of



Surface terminations along (110) plane of $\text{La}_{(1-x)}\text{Sr}_x\text{FeO}_3$:

Different surface terminations along (110) plane of $\text{La}_{(1-x)}\text{Sr}_x\text{FeO}_3$ are shown in Figure S4.

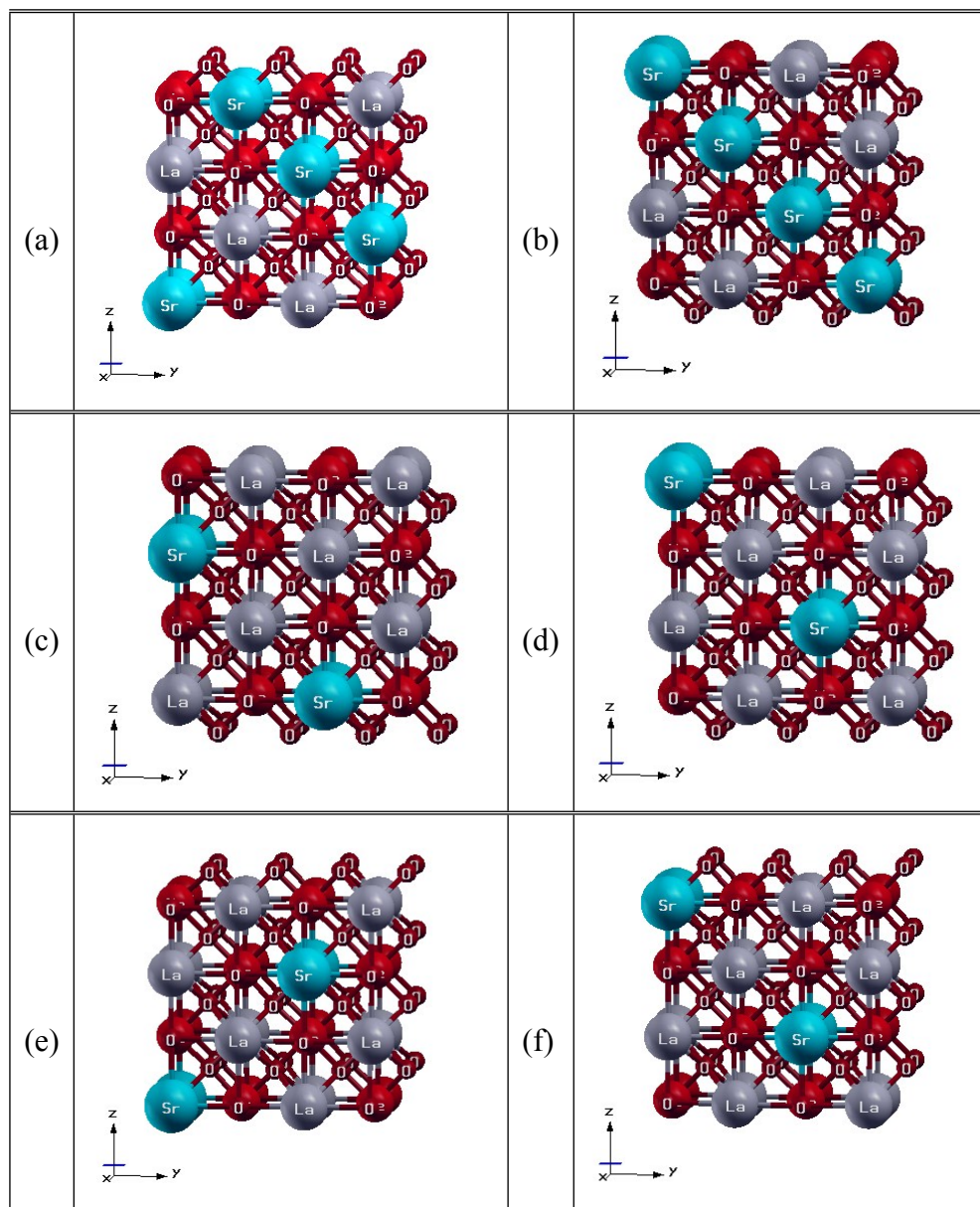


Figure S4: Surface termination along (110) facets of (a-b) $\text{La}_{0.5}\text{Sr}_{0.5}\text{FeO}_3$ and (c-f) $\text{La}_{0.75}\text{Sr}_{0.25}\text{FeO}_3$.

Surface oxygen vacancies:

The oxygen vacancy formation energies on various surface terminations for different extents of oxygen vacancy ($\delta = 0.125$ and 0.25) are shown in Figure S5. AO terminations proved to be most reluctant to create oxygen vacancies, while BO terminations and O-terminations are quite favorable.

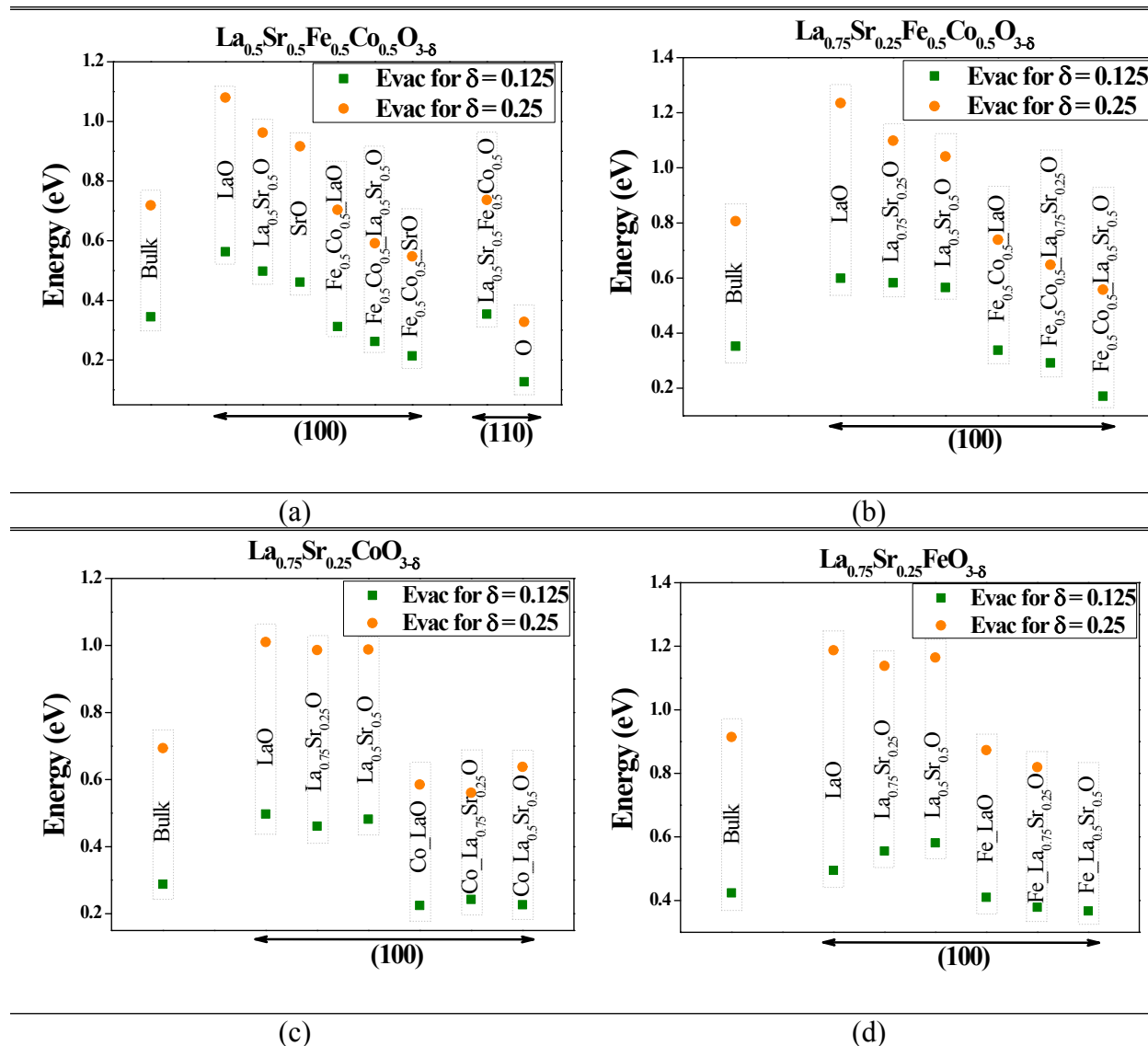


Figure S5 (a-d): Surface oxygen vacancy formation energy over various terminations for

(a) $\text{La}_{0.5}\text{Sr}_{0.5}\text{Fe}_{0.5}\text{Co}_{0.5}\text{O}_{(3-\delta)}$, (b) $\text{La}_{0.75}\text{Sr}_{0.25}\text{Fe}_{0.5}\text{Co}_{0.5}\text{O}_{(3-\delta)}$, (c) $\text{La}_{0.75}\text{Sr}_{0.25}\text{CoO}_{(3-\delta)}$ and

(d) $\text{La}_{0.75}\text{Sr}_{0.25}\text{FeO}_{(3-\delta)}$

DFT+U graphs for Surface Oxygen Vacancies

Surface oxygen vacancy formation energies along the (100) crystal facets of $\text{La}_{0.5}\text{Sr}_{0.5}\text{FeO}_3$ were calculated using the Hubbard U correction ($U = 2, 3$ and 4) as revealed in Figure S6.

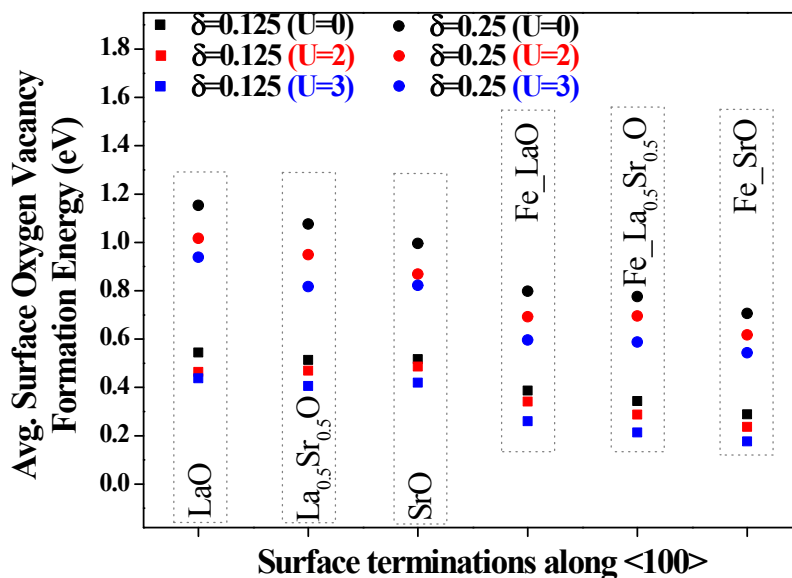


Figure S6. Surface oxygen vacancy formation energies along the (100) crystal facets of $\text{La}_{0.5}\text{Sr}_{0.5}\text{FeO}_3$ using DFT+U ($U = 2,3,4$)

Surface relaxations associated with oxygen vacancy formation:

Oxygen vacancy formation on the surface causes a major surface relaxation, thus, accounting for some trench like regimes on the surface. Figure S7 reveal some of the oxygen vacant surface terminations.

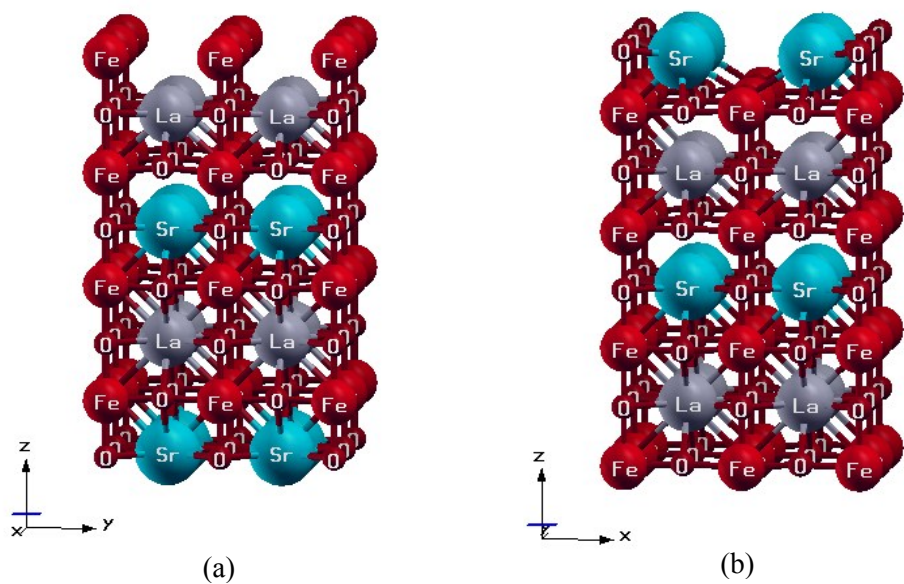


Figure S7 (a-b): Surface relaxations associated with oxygen vacancy formation on the surface terminations of for (a) $\text{La}_{0.5}\text{Sr}_{0.5}\text{FeO}_{(3-\delta)}$